Learning to see VOCs with Liquid Crystal Droplets

Susana I. C. J. Palma[1,2], José Frazão[4], Rita Alves[1,2], Henrique M. A. Costa[1,2], Cláudia Alves[1,2], Hugo Gamboa[3], Margarida Silveira[4], Ana C. A. Roque[1,2]

[1]*Associate Laboratory i4HB – Institute for Health and Bioeconomy*
[2]*UCIBIO – Applied Molecular Biosciences Unit, Department of Chemistry*
[3]*LIBPhys - Laboratory for Instrumentation, Biomedical Engineering and Radiation Physics*
NOVA School of Science and Technology, NOVA University of Lisboa, 2829-516 Caparica, Portugal
[4]*Institute for Systems and Robotics (ISR)*, Instituto Superior Técnico (IST), University of Lisbon, 1049-001 Lisbon, Portugal

{hma.costa, ran.alves, cma.alves}@campus.fct.unl.pt, {s.palma, h.gamboa, cecilia.roque}@fct.unl.pt, jose.l.frazao@tecnico.ulisboa.pt, msilveira@isr.tecnico.ulisboa.pt

***Abstract*—In hybrid gels with immobilized liquid crystal (LC) droplets, fast and unique optical texture variations are generated when distinct volatile organic compounds (VOCs) interact with the LC and disturb its molecular order. The optical texture variations can be observed under a polarized optical microscope or transduced into a signal representing the variations of light transmitted through the LC. We show how hybrid gels can accurately identify 11 distinct VOCs by using deep learning to analyze optical texture variations of individual droplets (0.93 average F1-score) and by using machine learning to analyze 1D optical signals from multiple droplets in hybrid gels (0.88 average F1-score).**

Keywords—liquid crystal; hybrid gels, image recognition; optical sensing

I. Introduction

Liquid crystals (LC) are soft materials with able to form dynamic stimuli-responsive supramolecular structures. When LC molecules are orderly assembled, they can alter the plane of polarized light, allowing light transmission through the material and generating interference patterns and colours (optical textures) observable under polarized optical microscopy (POM). Perturbation of molecular order results in alterations of the optical textures and, consequently, to changes in the intensity of light transmitted through the material. This is the basis to design chemical and biological sensing devices [1], including gas sensors, where LC work as optical probes with fast and reversible responses, low energy demand, operation at room temperature and tunable selectivity [2]. In hybrid gel films, LC droplets are embedded in a gel-like matrix composed by gelatin and ionic liquid [3]. The LC molecules are anchored perpendicularly to the interface, resulting in a radial configuration typically observed in POM as a Maltese cross optical texture (Fig 1). In the presence of different VOCs the LC radial configuration is rapidly disturbed and recovered when the VOC is removed (less than 20 s) (Fig. 1c). VOCs with different chemical functionalities interact preferentially with different components of the gel, resulting in different optical textures variations within the droplets [3]–[5]. Either POM or the light transmittance signal (Fig. 1d) can be used to monitor VOC interactions with the material and, since typical texture and signal patterns are observed for different VOCs, artificial intelligence can help to automatically identify the VOC by learning to recognize typical features of the LC responses [4], [6], [7]. We present two approaches for VOC recognition using distinct data formats extracted from hybrid gel films upon exposure to 11 VOCs representative of distinct chemical classes. The first approach is a Convolutional Neural Network pattern recognition system based the video analysis of the optical textures of individual LC droplets [8]. The second approach is a Support Vector Machine (SVM) classifier based on morphological features of the optical signals (light transmittance) collected from a region of hybrid gel with multiple droplets Both methodologies successfully leaned to identify the tested VOCs, further confirming the potential of hybrid gels for gas sensing either at the multi-droplet level, or at the single droplet level.

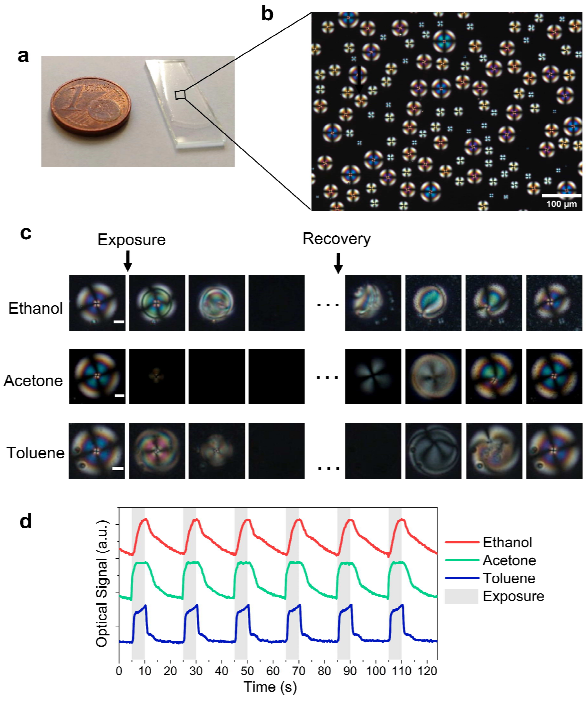

Fig. 1. Hybrid gels and their optical response to VOCs. (a) Gel spread over a glass slide. (b) POM micrograph taken with crossed polarizers, of a gel area before VOC exposure. (c) Optical textures of a LC droplet during one cycle of exposure (5 s) / recovery (15 s). Scale bar corresponds to 5 µm. (d) Optical signals of a sensing gel during 6 identical exposure (5 s) /recovery (15 s) cycles.

II. Materials and Methods

A. *Video-recordings of responses to VOCs*

Gelatin hybrid gels were prepared and spread as films over untreated glass slides [4] Each film was positioned inside a glass chamber placed in the stage of a polarising optical microscope (Zeiss Axio Observer. Z1/7, (Zeiss, Oberkochen, Germany). A VOC delivery system assembled

This work was supported by ERC funding under the EU Horizon 2020 research and innovation programme (SCENT-ERC-2014-STG-639123, 2014-2022) and by national funds from Fundação para a Ciência e Tecnologia, I.P. (research projects PTDC/BII-BIO/28878/2017 and PTDC/CTM-CTM/3389/2021, UCIBIO projects UIDP/04378/2020 and UIDB/04378/2020 and Associate Laboratory projects LA/P/0140/2020-i4HB and UIDB/50009/2020-LARSyS).

in-house was connected to the glass chamber and alternately pushed a VOC sample and clean air through the chamber in a cyclic way. To generate the VOC samples, room air was pumped through the headspace of a 30 mL vial containing 15 mL of pure solvent at 37 °C leading to VOC concentration of 12% - 15% (v/v) [4]. Each film was subjected to 5 consecutive cycles of exposure (5 s) and recovery (15 s, with clean air) with one of 11 VOCs (heptane, hexane, chloroform, toluene, dichloromethane, diethyl ether, ethyl acetate, acetonitrile, acetone, ethanol, and methanol). The alterations in the LC order within the droplets were video recorded in a single region of the gel film (Fig. 1a) using the microscope camera. One video per VOC was generated.

B. Video analysis

The droplets in each video were detected using an implementation of YOLOv3 network available on GitHub (https://github.com/wizyoung/YOLOv3_TensorFlow) with parameters optimized for our dataset of images [8]. YOLOv3 (You Only Look Once) is an algorithm that uses convolutional neural networks for object detection and classification [9]. The droplets were assembled in sequences, each of them corresponding to the textural transformations observed during a cycle of exposure to VOC and recovery with clean air. Then, a bidimensional convolutional neural network (2D CNN) combined with a Long Short Term Memory (LSTM) [10]–[12] was employed to extract features from the droplet sequences and perform the classification. The same 2D CNN is applied to every frame in the image sequence and extracts features that are then fed to the LSTM to learn time features for each sequence. The 2D CNN was composed by three sets of two convolutional layers (with ReLU activation) and a MaxPooling layer, totalling 9 layers. Padding was applied in the convolutional layers and there was a dropout layer before the final classification layer, a 11-unit softmax activation function (for 11 VOC Classification). Several values were tested for the parameters of this network [8]. To select the hyper-parameters, a grid search was performed [8]. The model was trained with the 'Adam' optimizer using Categorical Crossentropy as the loss function. A stacking ensemble [13] was used to aggregate the predictions made over the same data by 12 different base models of 2D CNN+LSTM corresponding to the total number of combinations of different hyper-parameter values (Table I). A Gaussian Naïve Bayes classifier was the meta-model of the stacking ensemble [8].

TABLE I. CNN MODEL PARAMETERS, WITH THE HYPER-PARAMETERS SHOWN IN BOLD.

Parameters	2D CNN + LSTM
Number of Filters	8, 16, 32
Filter Dimensions	**(3 × 3), (5 × 5), (7 × 7)**
Stride	1
Max-Pool window	2 × 2
Max-Pool stride	2
Dropout rate	0.5
Units FCL1	**16, 32**
Units LSTM	**16, 32**
Units Softmax	11

The original videos were split to generate the required training, validation and testing datasets. The 3 first exposure cycles to each VOC were selected for the training set, the fourth cycle for the validation set (to select the best hyperparameters and avoid overfitting) and the last one for the test set (to evaluate the classification performance).

C. Collection of optical signal responses to VOCs

Gelatin hybrid gels with the same formulation of those used for the video experiments were used as sensing materials in an in-house assembled optical signal acquisition device [4], [14]. The VOC delivery system used in the video experiments was connected to the acquisition device to generate identical VOC samples. Using this setup, 8 experiments were performed. In each experiment, multiple films were exposed sequentially to the 11 VOCs listed above [4]. The films were subjected to each VOC during 45 consecutive cycles of exposure (5 s) and recovery (15 s, with clean air). In total, optical signals from 20 independent gel films from 8 different batches were collected.

D. Optical signal analysis

After filtering noise and high fluctuations with a median filter and a 100-point sliding window smoothing filter from the *novainstrumentation* Python library (https://github.com/hgamboa/novainstrumentation), the full optical signals were split into individual cycles. As we are interested in analysing the shape rather than the intensity of the films' response to VOCs, the cycles were normalised. Fifteen morphological features (Table II) were extracted per cycle and used to build classification models based on a Support Vector Machines (SVM) classifier from *scikit-learn* Python library, with radial basis function kernel and hyperparameters C = 100 and $\gamma = 0.1$ [14].

TABLE II. FEATURES OF THE OPTICAL SIGNAL CYCLES

Number	Feature Description
1	Time to reach the minimum of the first derivative of the cycle
2	Minimum value of the first derivative of the cycle
3	Time to reach the maximum of the first derivative of the cycle
4	Maximum value of the first derivative of the cycle
5	Time to reach the maximum of the first half of the second derivative of the cycle
6	Maximum values of the first half of the second derivative of the cycle
7	Time to reach the minimum of the first half of the second derivative of the cycle
8	Minimum value of the first half of the second derivative of the cycle
9	Time to reach the maximum of the second half of the second derivative of the cycle
10	Maximum value of the second half of the second derivative of the cycle
11	Time to reach the minimum of the second half of the second derivative of the cycle
12	Minimum value of the second half of the second derivative of the cycle
13	Area under the cycle
14	Skewness
15	Kurtosis

Cycles from 6 experiments were used as training set and cycles from 2 experiments as testing set. All the possible combinations of training and testing sets were included by permuting the 8 available experiments. A confusion matrix

was generated considering the predictions made by each model (one model per combination).

RESULTS AND DISCUSSION

E. *VOC classification by video analysis*

Each gel film contained on average 130 droplets with diameters between 12 and 66 µm, all undergoing the same 5 VOC exposure cycles. The YOLOv3 model [8], was able to detect droplets in individual frames with an average precision of 0.97 in the testing dataset. There were 4295 sequences to train, 1368 to validate and 1345 to test the 2D CNN + LSTM models [8]. The ensemble model outperformed the single model by 3%, with an average F1-score of 0.93 (Table III), suggesting that the best hyper-parameters that were chosen for the single models are not the most suitable for every VOC or every droplet diameter. With the ensemble model there was a performance improvement for every VOC except ethyl acetate (F1-score 0.59) and dichloromethane (F1-score 76%). This might be related with the diameter of the droplets exposed to ethyl acetate, which was under 24 µm, the threshold above which we found better classifications[8]. The failures in the recognition of ethyl acetate also affect the F1-score of dichloromethane because most of the misclassified ethyl acetate sequences were wrongly classified as dichloromethane (Fig. 2a). The remaining VOCs were mostly correctly classified (accuracy higher than 0.95). These results suggest that the pattern of textural alterations of an individual droplet represent VOC fingerprints which could be used as VOC detectors. To further characterize this VOC classifier, the model could be tested with a test set comprising unseen droplet image sequences, taken from new videos.

TABLE III. CLASSIFICATION ON DROPLET IMAGE SEQUENCES TEST SET

VOC	F1-Score for 2D CNN+LSTM	
	Ensemble model	*Single model*
Acetone	1	0.981
Acetonitrile	0.962	0.887
Chloroform	1	0.977
Dichloromethane	0.763	0.834
Diethyl ether	0.96	0.803
Ethanol	0.991	0.978
Ethyl acetante	0.594	0.608
Heptane	1	1
Hexane	1	0.990
Methanol	1	0.989
Toluene	0.982	0.940
Average	**0.932**	**0.908**

F. *VOC classification with optical signals*

The optical signals of hybrid gel films (Fig 1a, 1b) are an alternative VOC detection method, relying on simpler hardware that measures the intensity of light transmitted through the gel films. As a film contains multiple droplets (Fig. 1b), the collected as signal is the cumulative effect of the LC disorganization patterns of individual droplets when exposed to the VOCs. Rich signal waveform patterns are generated in response to VOCs (Fig. 1d). The SVM classifier produced classifications with an average F1-score of 0.88, slightly lower than that of the video approach but still excellent. Several factors may justify the performance differences. The signals are a representation of the LC textural variations but lack information on colors. On the other hand, the signals dataset included more variability, which could decrease the performance. While videos were recorded in a single experiment and there was only one gel film per VOC, signals were obtained with 20 independent gel films per VOC, during 8 experiments performed in different days by different operators. We selected cycles from independent experiments for training and testing sets to test the ability of system to make predictions on new cycles based on past information. This is the closest approach to the concept of electronic nose. Correct classification rates between 0.76 and 0.99 were obtained (Fig. 2b), supporting the idea that the optical signals are a simple but rich representation that retains VOC-fingerprinting information. Two of the most misclassified VOCs, ethanol and methanol, are chemically similar, which might justify the confusion.

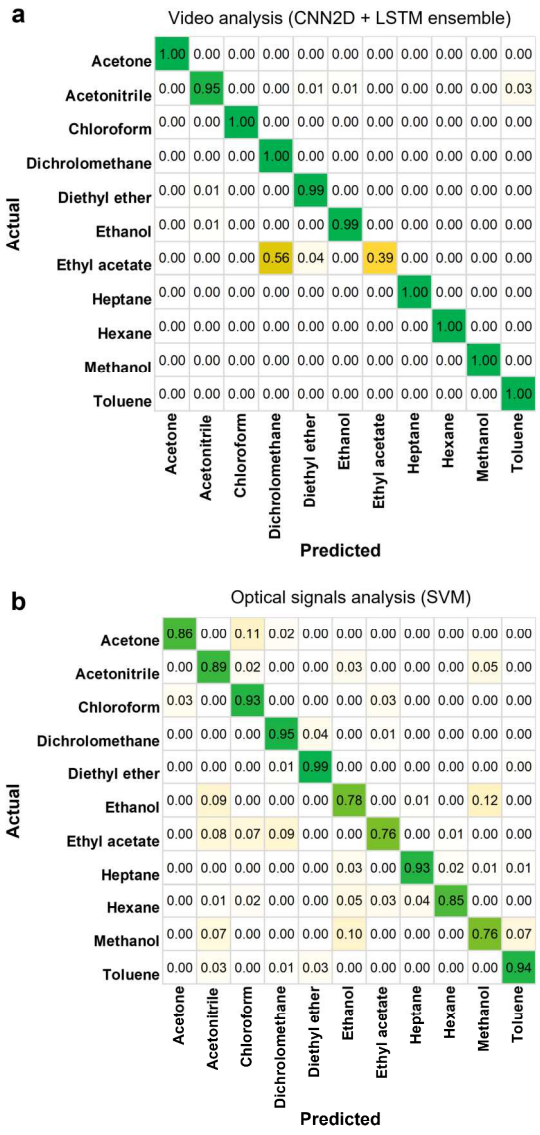

Fig. 2. Normalised confusion matrices representing the rates of correct (diagonal) and incorrect (off-diagonal) VOC classifications for (a) the video analysis (b) the optical signals analysis.

III. CONCLUSION

We present two alternative VOC pattern recognition approaches applicable to hybrid gas-sensing gels VOC

signals. The first one was the video analysis of the textural patterns of individual LC droplets. This is an entirely automated approach that takes advantage of the full extent of information carried by LC optical textures, namely morphological and colour changes along time. A deep learning stacking ensemble (2D CNN + LSTM) can learn an accurate model (0.93 F1-score) to detect 11 distinct VOCs. The second approach was based on a simpler representation of the LC optical responses – a 1D optical signal collected from a gel region with multiple LC droplets. A set of 15 known features extracted from the signals are sufficient for a SVM algorithm to learn a model to accurately (0.88 F1-score) detect the 11 VOCs. LC droplets respond fast (in less than 20 s) and are sufficient for VOC discrimination. The hybrid gel production is simple and scalable and so are the proposed CNN and SVM models. Our sensing platform is a versatile system where the transduction and pattern recognition methods can be adapted to the needs.

IV. REFERENCES

[1] R. J. Carlton *et al.*, "Chemical and biological sensing using liquid crystals.," *Liq. Cryst. Rev.*, vol. 1, no. 1, pp. 29–51, 2013.

[2] C. Esteves, E. Ramou, A. R. P. Porteira, A. J. Moura Barbosa, and A. C. A. Roque, "Seeing the Unseen: The Role of Liquid Crystals in Gas-Sensing Technologies," *Adv. Opt. Mater.*, vol. 8, p. 1902117, 2020.

[3] A. Hussain *et al.*, "Tunable Gas Sensing Gels by Cooperative Assembly," *Adv. Funct. Mater.*, vol. 27, no. 27, p. 1700803, 2017.

[4] C. Esteves *et al.*, "Effect of film thickness in gelatin hybrid gels for artificial olfaction," *Mater. Today Bio*, vol. 1, p. 100002, Jan. 2019.

[5] C. Esteves *et al.*, "Tackling Humidity with Designer Ionic Liquid-Based Gas Sensing Soft Materials," *Adv. Mater.*, vol. 34, no. 8, p. 2107205, Jan. 2022.

[6] Y. Cao, H. Yu, N. L. Abbott, and V. M. Zavala, "Machine Learning Algorithms for Liquid Crystal-Based Sensors," *ACS Sensors*, vol. 3, no. 11, pp. 2237–2245, Nov. 2018.

[7] A. D. Smith, N. Abbott, and V. M. Zavala, "Convolutional Network Analysis of Optical Micrographs for Liquid Crystal Sensors," *J. Phys. Chem. C*, vol. 124, no. 28, pp. 15152–15161, Jul. 2020.

[8] J. L. Frazão *et al.*, "Optical Gas Sensing with Liquid Crystal Droplets and Convolutional Neural Networks," *Sensors,* vol. 21, no. 8, pp. 2854, Apr. 2021.

[9] J. Redmon and A. Farhadi, "YOLOv3: An Incremental Improvement," *CoRR*, vol. abs/1804.0, 2018, [Online].

[10] S. Hochreiter and J. Schmidhuber, "Long Short-Term Memory," *Neural Comput.*, vol. 9, no. 8, pp. 1735–1780, Nov. 1997.

[11] Y. Lecun, Y. Bengio, and G. Hinton, "Deep learning," *Nature*, vol. 521, no. 7553. pp. 436–444, May 28, 2015.

[12] I. Goodfellow, Y. Bengio, and A. Courville, *Deep Learning*. MIT Press, 2016.

[13] L. I. Kuncheva, *Combining Pattern Classifiers: Methods and Algorithms*. NJ, USA: Wiley:Hoboken, 2014.

[14] G. Santos, C. Alves, A. C. Pádua, S. Palma, H. Gamboa, and A. C. Roque, "An optimized e-nose for efficient volatile sensing and discrimination," Proceedings of *BIODEVICES 2019*, pp. 36–46, 2019.